Microstructure and mechanics of crazes in oriented polystyrene

Nigel R. Farrar* and Edward J. Kramer
Department of Materials Science and Engineering and the Materials Science Center, Cornell University, Ithaca, NY 14853, *USA*
(*Received* 24 *July* 1980; *revised* 10 *September* 1980)

Crazes are produced in oriented polystyrene (PS) thin films, bonded to copper grids, by applying a tensile strain to the grids in directions parallel to, or perpendicular to the axis of molecular orientation. The crazes produced by straining parallel to the molecular orientation direction (parallel crazes) have a higher fibril volume fraction (v_f=0.45) than crazes in unoriented PS (v_f=0.25). The crazes produced by straining perpendicular to the molecular orientation direction (perpendicular crazes) have a much lower fibril volume fraction (v_f=0.05) than either parallel crazes or crazes in unoriented PS. These differences in fibril volume fraction are reflected in the micromechanics of the crazes. Perpendicular crazes show a higher stress concentration at the craze tip and a larger stress relief behind the craze tip than do the parallel crazes. The fibrils in long perpendicular crazes break down readily to form cracks whereas no parallel craze breakdown at similar strains is observed. These differences in craze microstructure and micromechanics are believed responsible for the marked anisotropy in the fracture properties of oriented glassy polymers.

INTRODUCTION

It is now well established that molecular orientation in a polymeric glass can lead to large anisotropy in the fracture behaviour[1-6], e.g. high fracture stresses parallel to the orientation direction and low fracture stresses transverse to it. Since many fabrication processes, e.g. injection moulding and extrusion, introduce some molecular orientation, the resulting anisotropy in fracture properties is a matter of some practical concern. At first, it would seem possible to attribute this anisotropy to the anisotropy of Young's modulus E, since the critical stress intensity factor for crack propagation is given by

$$K_{I_c} = \sqrt{G_{I_c} E}$$

where G_{I_c} is a critical strain energy release or energy required per unit area crack advance. Measurements of Young's modulus of the glass[7-9], however, show that the anisotropy in E is much smaller than the anisotropy of fracture properties, particularly in polystyrene[10]. Hence, it appears that the fracture anisotropy originates either from an anisotropy in initial natural flaw sizes or from an anisotropy of G_{I_c}.

In unoriented glassy polymers fracture involves the prior nucleation and growth of crazes in response to the tensile stress. These defects consist of interconnected voids and fine polymer fibrils, ~6 nm in diameter and ~0.25 volume fraction[11], which span from one craze-bulk polymer interface to the other. Crazes taper in thickness from ~5–10 nm near the craze tip, to ~1 μm near the craze base. When a crack forms, it invariable does so by breakdown of the fibril structure within the craze, so that the natural flaw in this case is not a static preexisting crack, but one which develops over time as a result of craze formation and breakdown[12-19]. However, once the crack has propagated beyond the confines of the original craze, the high stresses at the crack tip result in the generation of new crazes ahead of the crack tip, and the plastic work done during their formation gives rise to the relatively large G_{I_c}'s measured for these polymers.

Given this background, it appears that the anisotropy of fracture properties in oriented polymeric glasses may have its origin in differences in the microstructure and mechanical properties of crazes formed at various directions relative to the orientation direction in the glass. However, there have been few previous investigations of crazes in oriented glassy polymers[20-22]. The most definitive study was one by Beardmore and Rabinowitz[22] on oriented poly(methyl methacrylate) (PMMA). They showed that crazes formed at higher stresses when the tensile axis was parallel to the molecular orientation direction M, than when the axis was normal to M, and that fracture occured at stresses above the minimum stress for crazing in all cases. They also showed that the overall craze morphology depended on the stress direction relative to the orientation axis, with many short crazes formed before fracture when the stress was parallel to M, and only a few long crazes formed before fracture when the stress was perpendicular to M. In this paper we show that crazes formed by stressing parallel to M and perpendicular to M have strikingly different microstructures and mechanical properties. These observed differences allow the construction of natural explanations for both the results of Beardmore and Rabinowitz and the anisotropy of fracture properties in oriented polymeric glasses.

EXPERIMENTAL

Films were prepared from thermally polymerized atactic polystyrene (PS) which had a weight average molecular

* Present address: Raychem Corporation, 300 Constitution Dr., Menlo Park, CA 94025, USA

0032-3861/81/050691-08$02.00

weight $\bar{M}_W = 250\,000$ and a polydispersity index $\bar{M}_W/\bar{M}_N = 2.3$. This polymer, which was free of the usual additives found in commercial PS, such as mineral oil, was kindly provided by Dr. Robert Bubeck of Dow Chemical Company.

Thin films of uniform thickness were produced on substrates by drawing these from a PS–toluene solution at a constant rate. The film thickness was controlled by changing the solution viscosity by altering its concentration. For transmission electron microscope (*TEM*) studies, films should be less than 1 μm thick. The films were drawn from solution to an initial thickness that was calculated to thin to the desired value during the orientation process. Since the initial thickness was in the range of 1–10 μm, these films required mechanical support during the elevated temperature orientation process. Ultra high molecular weight ($\bar{M}_W \approx 10^7$) linear polyethylene (PE) was chosen as a drawing substrate, as this material enabled large draw ratios to be achieved at temperatures above the glass transition temperature of PS.

Strips of PE (25 mm long, 13 mm wide, 1.6 mm thick) were pulled from the PS solution to produce the initial film, and glass slides were also pulled from the same solution. The latter were used to measure the initial film thickness by optical interference microscopy. The coated PE strips were mounted in a tensile straining device which was heated in an oven to temperatures between 105 and 125°C. After thermal equilibrium had been reached, the strips were drawn rapidly to various extension ratios and quenched by removing the straining rig from the oven and plunging it into cold water.

In order to enable the molecular orientation produced in the PS films to be characterized, some PE strips were coated with two films of PS (one at each end of the strip). One of these was thin enough for *TEM* studies and the other was thick enough to allow birefringence measurements to be made.

After drawing and quenching, the PS films were stripped from the PE using polyacrylic acid (PAA). The PS–PAA composite was then placed on the surface of a water bath. The PAA dissolved leaving the oriented PS film floating on the surface of the water. At the same time, the grid bars of a well annealed copper mesh strip were coated with PS by dipping in a low concentration PS solution. The toluene was allowed to evaporated until the PS on the grid bars became tacky. A dry copper mesh was used to pick up the oriented PS film from the water surface and then used to transfer the film to the tacky PS grid. If the PS solution on the grid bars was allowed to dry to the correct degree of tackiness, a bond was formed between the PS film and the grid bars, without altering the molecular orientation in the film. During the process of picking up the films from the water surface, care was taken to align the molecular orientation direction of the film with one of the axes of the grid.

Crazes were produced by straining the copper grids in directions parallel to, or perpendicular to the molecular orientation direction of the films. The strain in the PS film was maintained after the grid was removed from the straining device due to the fact that the copper grid bars, which deformed plastically under the initial strain, exhibited negligible strain recovery. Crazes usually nucleated and grew from small dust particles of ~ 1 μm diameter which acted as stress concentrators in the films. Grid squares containing isolated crazes suitable for analysis were cut from the mesh and examined in the transmission electron microscope. Following the procedure established by Lauterwasser and Kramer[23], electron micrograph sequences were taken along the length of the selected craze. The volume fraction v_f of polymer fibrils in the craze was determined locally from microdensitometer measurements of the optical densities φ in regions of the micrograph corresponding to the solid film, a hole through the film, and the craze by using the equation[23]:

$$v_f = 1 - \frac{\ln(\varphi \text{ craze}/\varphi \text{ film})}{\ln(\varphi \text{ hole}/\varphi \text{ film})} \tag{1}$$

The craze thickness profile $T(x)$ was also measured from the micrographs (x is the distance along the craze) so that the craze surface displacement profile $w(x)$ could be obtained from[23]:

$$w(x) = \frac{T(x)}{2}(1 - v_f(x)) \tag{2}$$

STRESS ANALYSIS

Because of its large length to thickness ratio, a craze may be modelled as a loaded planar slit in a linear elastic sheet. For an isotropic sheet, the normal stresses on the surface of the craze $S(x)$ may be found conveniently using the Fourier transform method of Sneddon[24], i.e.

$$S(x) = \Delta S(x) + \sigma_\infty \tag{3}$$

where

$$\Delta S(x) = -\frac{2}{\pi}\int_0^\infty \dot{p}(\xi)\cos(x\xi)\,\mathrm{d}\xi \tag{4}$$

and

$$\dot{p}(\xi) = \frac{\xi E^*}{2}\int_0^a w(x)\cos(x\xi)\,\mathrm{d}x \tag{5}$$

Here, a is half the total craze length (tip to tip), σ_∞ is the tensile stress applied (normal to the craze) at a large distance from the craze plane and E^* is an isotropic modulus ($E^* = E$, Young's modulus, for plane stress and $E/(1-\nu^2)$, where ν is Poisson's ratio, for plane strain).

The stress field of the craze may also be modelled by considering the craze surface displacements due to a continuous distribution of dislocations of infinitesimal Burgers vector[25,26]. In the case of a craze, the dislocations correspond to a row of edge dislocations, shown schematically in *Figure 1*, lying in the z direction, with Burgers vectors b in the y direction. From dislocation theory $\Delta S(x)$ (to be substituted in Equation 3) is found for an isotropic sheet by summing the stresses σ_{yy} due to all the dislocations. The stresses σ_{yy} for a single dislocation are given by:

$$\sigma_{yy} = \frac{E^* b}{4\pi x} \text{ at } y = 0 \tag{6}$$

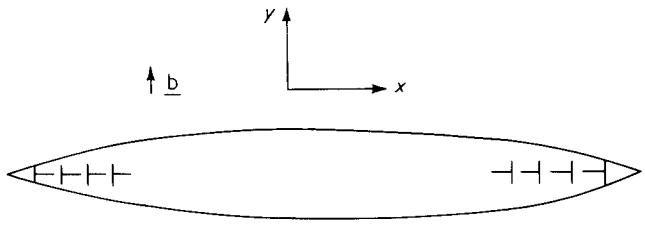

Figure 1 Schematic representation of the continuous dislocation distribution model for a craze

and the summation results in:

$$\Delta S(x)=\frac{-E^*}{2\pi}\int_0^a \frac{w'(x')\mathrm{d}x'}{(x-x')} \tag{7}$$

where

$$w'(x)=\frac{\mathrm{d}w}{\mathrm{d}x}$$

For an elastically anisotropic sheet these relations no longer apply. However, if there is isotropy about the draw direction, the symmetry is the same as that of a hexagonal crystal (with c axis = draw direction). The stresses, for x oriented parallel to the draw (orientation) direction, are given by the matrix representation in terms of the usual stiffness constants (C's) and the strains (ε's).

$$\begin{pmatrix}\sigma_{xx}\\ \sigma_{yy}\\ \sigma_{zz}\\ \sigma_{yz}\\ \sigma_{xz}\\ \sigma_{yx}\end{pmatrix}=\begin{pmatrix}C_{11} & C_{12} & C_{12} & 0 & 0 & 0\\ C_{12} & C_{22} & C_{23} & 0 & 0 & 0\\ C_{12} & C_{23} & C_{22} & 0 & 0 & 0\\ 0 & 0 & 0 & \frac{1}{2}(C_{22}-C_{23}) & 0 & 0\\ 0 & 0 & 0 & 0 & C_{66} & 0\\ 0 & 0 & 0 & 0 & 0 & C_{66}\end{pmatrix}\begin{pmatrix}\varepsilon_{xx}\\ \varepsilon_{yy}\\ \varepsilon_{zz}\\ \varepsilon_{yz}\\ \varepsilon_{xz}\\ \varepsilon_{yx}\end{pmatrix}$$

The stress due to a single dislocation with the geometry shown in *Figure 1* is given by[27]:

$$\sigma_{yy}=(\bar{C}_{11}+C_{12})\left[\frac{C_{66}(\bar{C}_{11}-C_{12})}{C_{11}(\bar{C}_{11}+C_{12}+2C_{66})}\right]^{1/2}\frac{b}{2\pi}\frac{1}{x}\ \text{at}\ y=0 \tag{8}$$

where $\bar{C}_{11}=\sqrt{C_{11}C_{22}}$. This geometry corresponds to the crazes produced by straining perpendicular to the orientation axis; for crazes produced by straining parallel to the orientation axis, C_{22} should be substituted for C_{11} in Equation 8. Comparing Equation 6 with Equation 8 it is clear that the anisotropic sheet responds as if it has an effective Youngs modulus E^* given by:

$$E^*=2(\bar{C}_{11}+C_{12})\left[\frac{C_{66}(\bar{C}_{11}-C_{12})}{C_{11}(\bar{C}_{11}+C_{12}+2C_{66})}\right]^{1/2} \tag{9}$$

Since the distributed dislocation method and the Fourier transform method are mathematically equivalent, either one may be used to compute the stresses on the craze surface in the anisotropic films, provided only that the corrected value of E^*, computed from the stiffness constants of the anisotropic sheet, is used. Because the Fourier transform method is more convenient for numerical computation, Equations 3–5 with the correct E^* have been used for finding the surface stresses.

The room temperature stiffnesses of oriented polystyrene have been measured using a ultrasonic-critical angle method, by Wright, Faraday, White and Treloar[10]. They found that surprisingly little elastic anisotropy developed even after large orientations were achieved. For example, at their highest orientation, which corresponds to a birefringence of -13×10^{-3}, the effective plane stress modulus is $E_0^*=2.85$ GPa for a tensile stress parallel to (and craze perpendicular to) the orientation direction, and the plane stress modulus is $E_{90}^*=2.73$ GPa for a tensile stress perpendicular to (and craze parallel to) the orientation direction. These values have been corrected to account for the difference between the long time scale (~1 day) of the crazing experiment and the short time scale of the ultrasonic measurement (~0.25 μs), and are to be compared to a 'static' isotropic Young's modulus of PS of 2.76 GPa. Since the birefringence of the films containing the crazes analysed here is also -13×10^{-3}, it is clear that the correction required for elastic anisotropy of the films is very small ($<3\%$).

RESULTS

Craze morphology and microstructure

Crazes are observed to form in the oriented films after straining the grids both parallel to the orientation direction (these we call 'parallel' crazes since the orientation direction is parallel to the axes of fibrils in the craze) and perpendicular to the orientation direction (these we call 'perpendicular' crazes). In both cases the crazes form on the plane normal to the tensile stress, a result which is to be expected both from symmetry and the prior experiments of Beardmore and Rabinowitz on PMMA. The morphology and microstructure of the parallel crazes are strikingly different from those of the perpendicular crazes, and both differ from the morphology and microstructure of crazes in unoriented PS films. After straining parallel to the orientation axis a large number of short and thin crazes are nucleated. Applying the same strain perpendicular to the orientation axis produces a much smaller number of long, wide crazes. This result is also in qualitative agreement with the observations of Beardmore and Rabinowitz on oriented PMMA.

The most remarkable differences, however, are observed when the fibril microstructures of the two orientations of crazes are examined in the *TEM*. The microstructures of the perpendicular crazes and the parallel crazes in regions just behind the craze tip are compared in *Figure 2*. The 'mature' craze fibril structures (in regions closer to the craze centre) of both perpendicular crazes and parallel crazes are shown in *Figure 3*. Clearly, the perpendicular crazes have a much smaller volume fraction of fibrils v_f than do the parallel crazes. Quantitative measurements of v_f in mature regions of both types of craze are made using microdensitometry and are shown in *Table 1*. A value of $\simeq0.05$ is measured consistently in perpendicular crazes, which is much less than the average value found by Lauterwasser and Kramer ($v_f\simeq0.25$) for crazes in unoriented PS, and which in turn is substantially less than the fibril volume fraction, $v_f\simeq0.45$, measured in the parallel crazes. The Table also shows that the ratio of maximum craze thickness to total craze length is much greater for perpendicular than for parallel crazes. Large

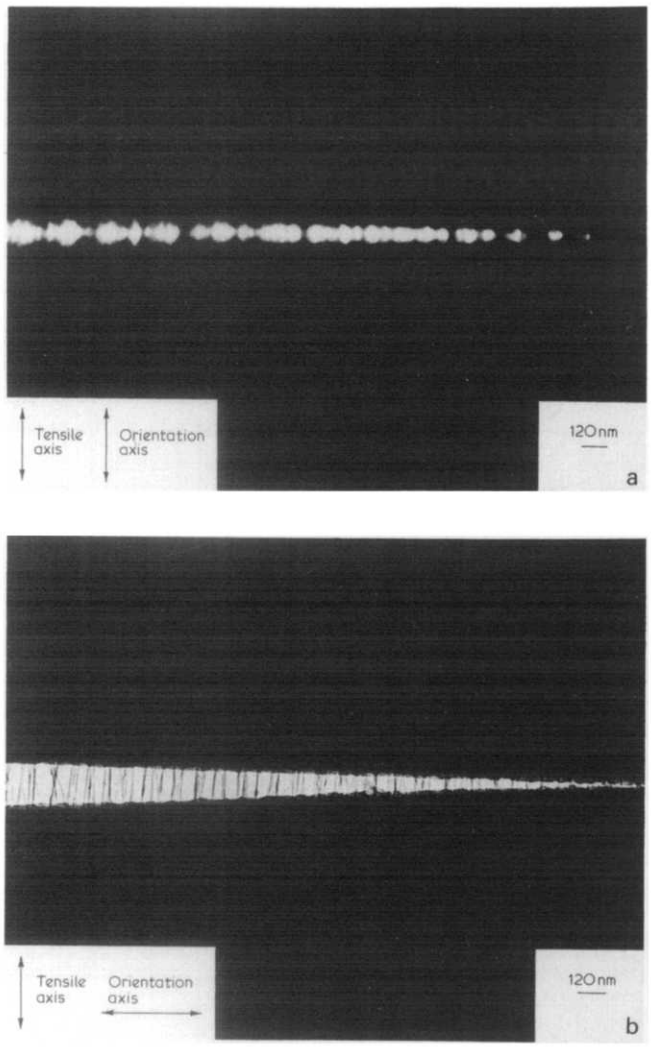

Figure 2 Transmission electron micrographs of craze tips in oriented polystyrene. The tensile axis is (a) parallel to the orientation direction and (b) perpendicular to the orientation direction

values of this ratio are associated with small values of craze load bearing capacity (average values of S produced by the craze fibrils). It would appear that the parallel crazes are stronger than the perpendicular crazes, in agreement with qualitative expectations after viewing the fibril microstructures of the two crazes and also the quantitative stress analysis of the following section. Another aspect of the weakness of the perpendicular crazes is also apparent from our observations that the fibril structure in the centre of very long crazes very often breaks down to form a crack. In such cases the only fibrils left intact are those in the craze ahead of the crack tip. Such broken crazes are fairly common in films strained perpendicular to the orientation direction but are never observed at the same strain level in the PS films strained parallel to the orientation direction.

The fibril diameter distribution for the perpendicular crazes is comparable to that for crazes in unoriented PS, where a mean diameter of 6 nm and range from 4 to 10 nm is found[11]. In the perpendicular crazes the fibril diameters range from about 4 to 20 nm. However, some of the larger fibrils may be associated with skins, near the film surfaces, which are drawn under plane stress conditions. Such skins are observed in crazes in unoriented PS, but the number of resulting fibrils is an insignificant portion of the total. The fibril structure in the parallel crazes appears to be much coarser, characterized by an average fibril diameter of about 40 nm. However, this figure could be smaller due to the effects of the very high density and strongly overlapping nature of the fibril structure in these crazes on measurements from the *TEM* image. Small angle X-ray scattering from crazes in bulk samples, which has been used to confirm measurements of fibril diameters in thin films[28], would be useful in determining whether these apparent diameters are correct.

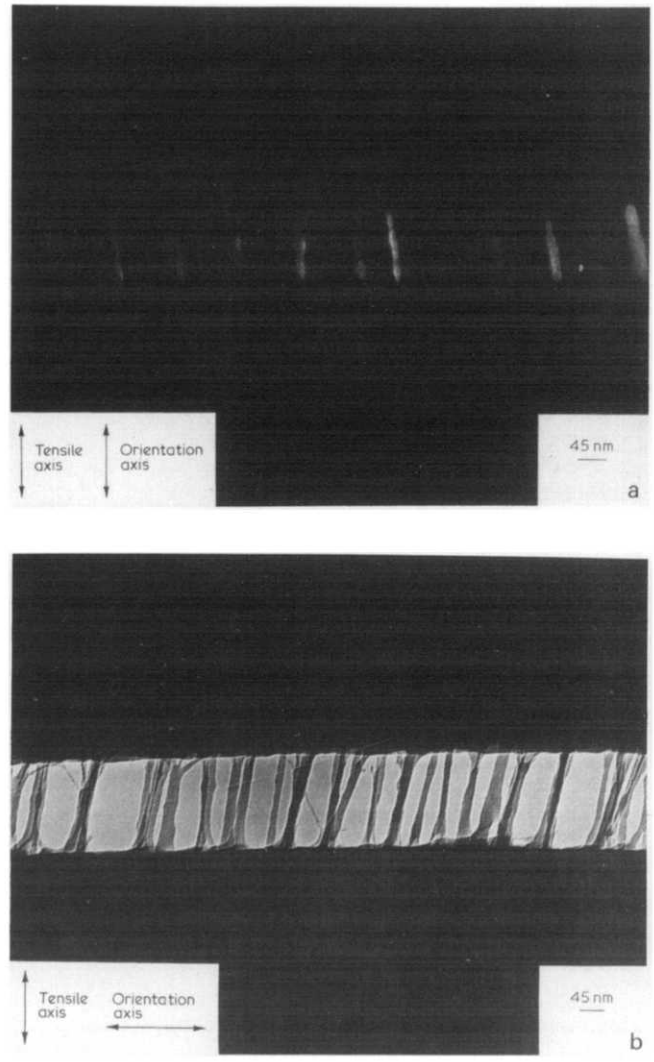

Figure 3 Transmission electron micrographs of the centre region (well away from the tip) of crazes in oriented polystyrene. The tensile axis is (a) parallel to the orientation direction, and (b) perpendicular to the orientation direction

Table 1 Microstructural measurements on crazes in oriented and unoriented PS

	Parallel	Unoriented	Perpendicular
Average fibril volume fraction	0.45	0.25	0.05
Average craze thickness/length ratio	0.010	0.005	0.080
Craze thickness (μm)	0.05–0.90	0.5	0.40–4.0
Crack length (μm)	3.0–90.0	100.0	6.0–>500

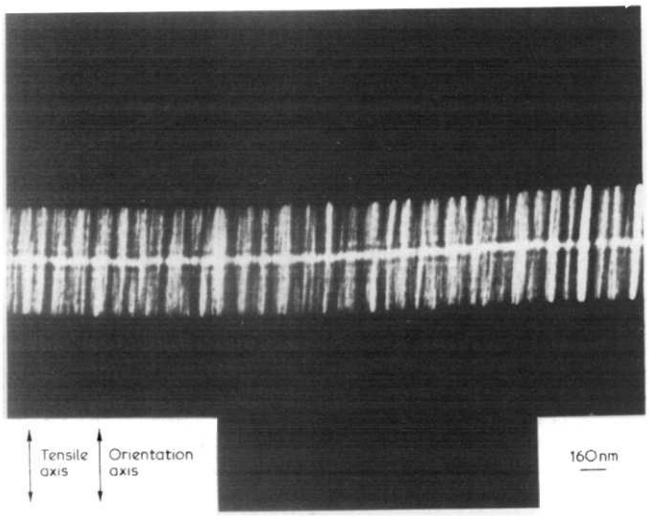

Figure 4 Transmission electron micrograph of the centre region of a craze in oriented polystyrene. The tensile axis and orientation direction are parallel

There is one final difference between the microstructures of parallel and perpendicular crazes. Whereas the parallel crazes usually have a midrib (a region of lower fibril volume fraction v_f along the centre of the craze), as illustrated in *Figure 4*, no midrib is observed in the perpendicular crazes. The midrib has been attributed to the drawing of fibrils from the craze-matrix interface at the high surface stresses which usually exist just behind the craze tip[23]. The higher stresses result in higher draw ratios for these regions of the fibril structure when compared to regions drawn from the craze surface at the lower stress that exist well behind the craze tip. If the craze thickens, not only by surface drawing of fibrillar material but also by fibril creep, one might expect the differences, between fibril material drawn behind the craze tip and material drawn further back from the tip, to be much less or erased entirely. If fibril creep were an important mechanism of craze thickening, the largest diameter fibrils would be observed just behind the craze tip, even though the stress is highest there, and as the craze thickens by creep of the fibrils, these will begin to break down in the thicker regions of the craze. A detailed analysis of the perpendicular craze in *Figure 2* shows that both these features are present. It seems likely, therefore, that the absence of a midrib in the perpendicular craze is due to the fact that fibril creep makes an important contribution to craze thickening, a contribution which is present in neither the parallel crazes nor crazes in unoriented PS[23]. In turn, the increased importance of fibril creep may imply the absence of an effective strain hardening mechanism for the fibrils in the perpendicular craze.

Craze micromechanics

Thickness profiles $T(x)$ for typical parallel and perpendicular crazes are shown in *Figure 5*. A short perpendicular craze has been selected so that an isolated craze with no fibril breakdown in its centre can be analysed. Longer perpendicular crazes exhibit either fibril breakdown, or grow from the grid bars. The corresponding displacement profiles computed from Equation 2 are shown in *Figure 6*. Whereas $2w(x)$ is slightly more than half $T(x)$ for the parallel craze, it is almost equal to $T(x)$ for the perpendicular craze, reflecting the differences in $v_f(x)$ between the two crazes.

The change in surface stresses $\Delta S(x)$, due to the craze opening alone, is computed from $w(x)$ using Equations 4 and 5, and these profiles are displayed in *Figure 7*. These are stresses that would act to keep the craze open in the absence of the applied tensile stress σ_∞. The total surface stress is $S(x)=\Delta S(x)+\sigma_\infty$, so that positive values of ΔS represent enhancement of the applied stress and negative values of ΔS represent stress relief. The ΔS values, which depend only on $w(x)$ and E^*, are known with more accuracy than σ_∞, which must be estimated from the tensile strain applied to the grid or from the opening displacements of a crack in another grid square. Because imperfections in the bonding of the grid affect the above estimates of σ_∞, these may be as much as 30% too high, whereas the ΔS values are known to $\pm 2\%$. The σ_∞ estimates are $\sigma_\infty \simeq 90$ MPa for the perpendicular craze and $\sigma_\infty \simeq 290$ MPa for the parallel craze, which correspond to applied strains of about 3 and 10% respectively.

Although the shapes of the $\Delta S(x)$ profiles are qualitatively similar to those obtained for crazes in unoriented PS, the differences in craze structure produce large quantitative differences in the micromechanics. In particular the parallel craze shows much less stress relief (less negative values of ΔS) behind the craze tip than does the

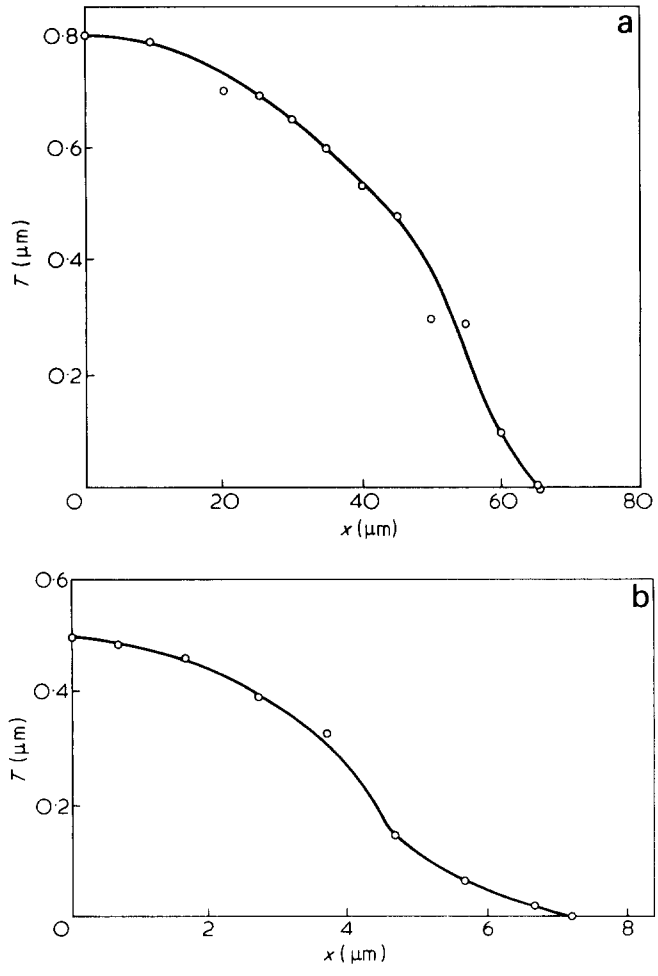

Figure 5 Thickness profiles for crazes in oriented polystyrene. The tensile axis is (a) parallel to the orientation direction and (b) perpendicular to the orientation direction

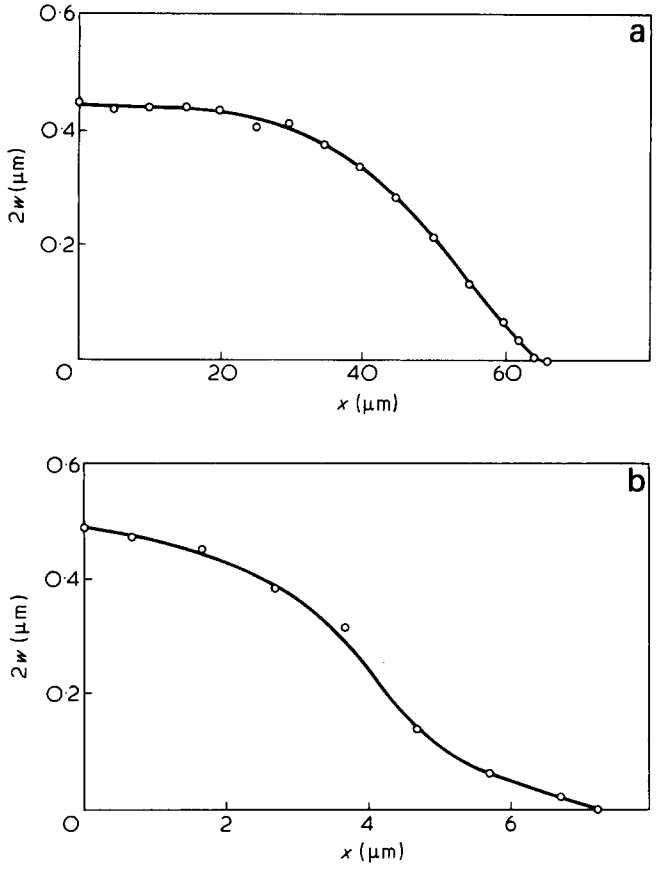

Figure 6 Opening displacement profiles for crazes in oriented polystyrene. The tensile axis is (a) parallel to the orientation direction and (b) perpendicular to the orientation direction

perpendicular craze. Clearly, the fibril structure of the parallel craze, with its high v_f, can support more load than that of the sparsely fibrillated perpendicular craze. The much smaller stress concentration at the tip of the parallel craze similarly results from the higher load bearing capacity of its dense fibril structure. The parallel craze is much less like a crack than is the perpendicular craze. However, the stress profile behind the tip of the perpendicular craze is rather irregular. This irregularity (in particular the peak in ΔS behind the craze tip) is thought to result from the small size of the craze analysed and the details of its fibril structure shown in *Figure 8*. Instead of the forces due to the fibrils being averaged over a short distance along the craze boundary, as they would be in a craze with a dense fibril structure, the tractions exerted by individual fibrils become important when there are very few of them. The peak in surface stress behind the craze tip corresponds well to the position of the large fibril marked at A in *Figure 8*.

The extension ratio profile $\lambda(x)$ of the fibrils ($\lambda = 1/v_f$) for the parallel craze is shown in *Figure 9*. The λ is approximately constant over most of the craze, increasing only just behind the craze tip. Since craze thickening by fibril creep would result in an increasing extension ratio with distance behind the craze tip, it may be concluded that, as for crazes in unoriented PS[23], craze thickening by fibril creep is not the major thickening mechanism for parallel crazes. However, since the mechanism of surface drawing naturally gives rise to such a $\lambda(x)$ profile[23], it appears that, as for crazes in unoriented PS, the thickening mechanism in the parallel crazes is surface drawing. Although microdensitometer measurements of the $\lambda(x)$ profile for the sparsely fibrillated perpendicular craze are not meaningful, measurements of fibril diameters in various regions of the craze imply that fibril creep is a more important mechanism for the thickening of perpendicular crazes.

Implications of the fracture of oriented polymers

Figure 10 shows the fracture stress σ_f (no pre-crack) of oriented PS, tested by straining both parallel and perpendicular to the molecular orientation axis, plotted as a function of birefringence (degree of molecular orientation), from the work of Curtis[2]. The σ_f parallel to the orientation direction increases, and the σ_f perpendicular to the orientation direction decreases with increasing molecular orientation. Knowing that breakdown of preexisting crazes is the first step in the nucleation of a crack in unoriented PS, these changes in oriented PS may be rationalized. Stressing parallel to the orientation direction produces crazes prior to fracture which have a large v_f and are resistant to fibril breakdown up to relatively high stresses. However, stressing perpendicular to the orientation direction produces crazes which have a very low fibril volume fraction and which are converted into cracks at quite low stresses by breakdown of the very sparse fibril structure. Not only the conditions necessary to nucleate a crack but also the critical strain energy release rate G_{I_c} for crack propagation will be different for

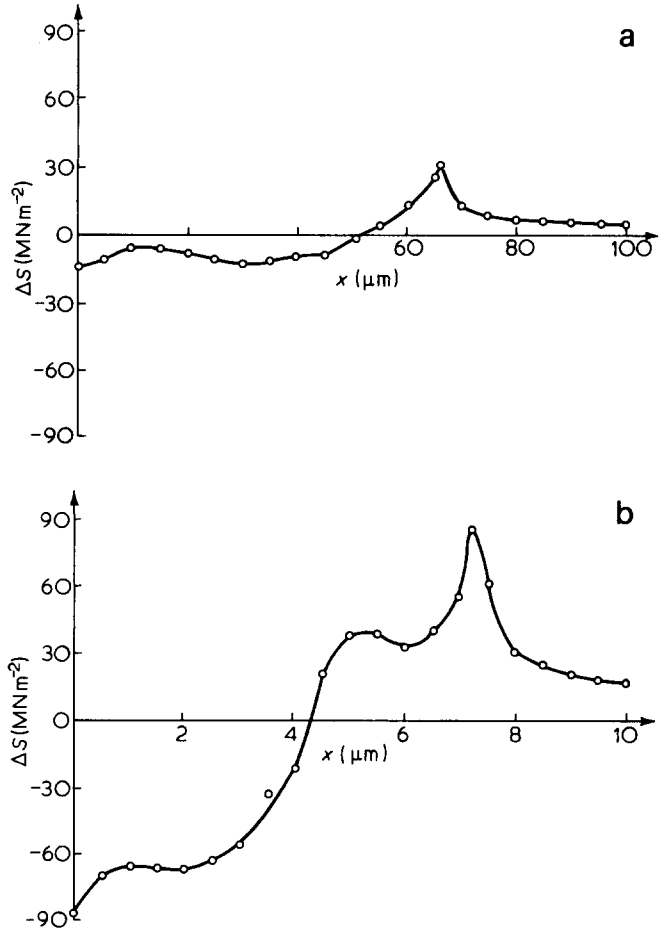

Figure 7 Surface stress profiles for crazes in oriented polystyrene. The tensile axis is (a) parallel to the orientation direction and (b) perpendicular to the orientation direction. The craze tips are at (a) 66.0 μm (b) 7.2 μm

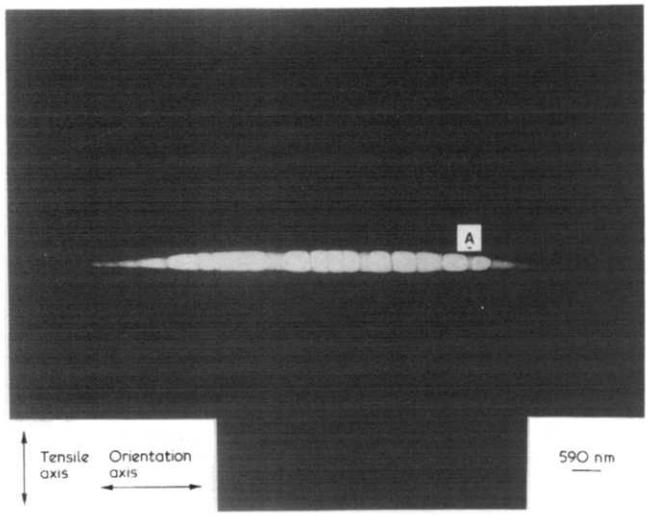

Figure 8 Transmission electron micrograph of a craze in oriented polystyrene. The tensile axis is perpendicular to the orientation direction

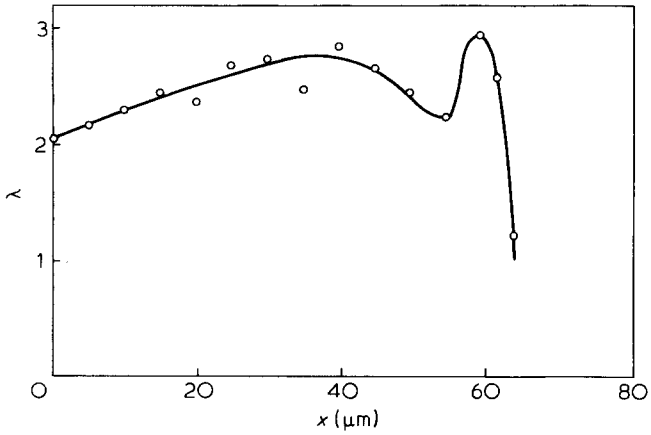

Figure 9 Variation of fibril draw ratio along the length of a craze in oriented polystyrene. The tensile axis is parallel to the orientation direction. The craze tip is at 66.0 μm

the different directions of stressing, since G_{I_c} is the plastic work per unit area involved in craze formation at the crack tip. For crack propagation, with a craze of constant length at its tip, G_{I_c} can be written as:

$$G_{I_c} = 2\int_0^{w_c} S(w)\mathrm{d}w \qquad (10)$$

where $S(w)$ is the surface stress corresponding to the surface displacement at a particular position along the craze and w_c is the craze surface displacement at the crack tip. If, as in a perpendicular craze, ΔS is large and negative over most of the craze, S is small and G_{I_c} would be smaller than for a parallel craze, for which both S and w_c are expected to be larger. Measurements of G_{I_c} in oriented PS[1,2,4] confirm these expectations by showing a similar trend to the σ_f data in *Figure 10*, although it is not as dramatic. Therefore, it seems likely that the differences in craze microstructure and micromechanics observed here underlie the anisotropy of both σ_f and G_{I_c} for oriented glassy polymers.

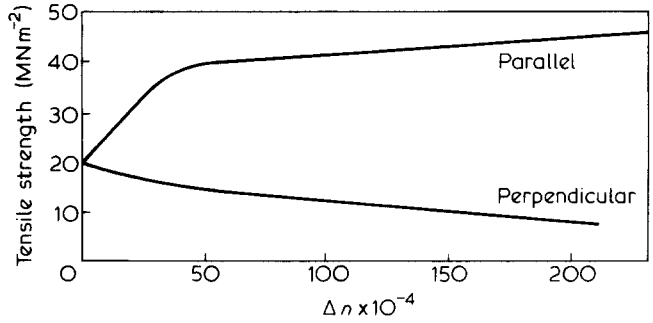

Figure 10 Variation of the tensile strength with orientation in polystyrene, tested parallel and perpendicular to the orientation direction (after Curtis[2])

CONCLUSIONS

The conclusions of this investigation may be summarized as follows:

(1) At similar tensile strain levels parallel crazes are smaller and more numerous than perpendicular crazes.

(2) The fibril volume fraction in parallel crazes is much greater than that in perpendicular crazes.

(3) The stress concentration near the craze tip, and stress relief in the craze base, are much greater in perpendicular crazes than in parallel crazes, i.e. parallel crazes are stronger.

(4) Crazes in unoriented PS show fibril volume fractions and surface stress profiles between these two extremes.

(5) This anisotropy in craze microstructure and micromechanical properties underlies the anisotropy in the fracture properties of oriented glassy polymers.

ACKNOWLEDGEMENTS

The financial support of the Cornell Materials Science Center which is funded by the National Science Foundation is greatly appreciated. We also thank Dr. Robert A. Bubeck of Dow Chemical Company for providing a generous supply of polydisperse polystyrene unadulterated with mineral oil.

REFERENCES

1 Broutman, L. J. and McGarry, F. J. *J. Appl. Polym. Sci.* 1965, **9**, 609
2 Curtis, J. W. *J. Phys. D.-Appl. Phys.* 1970, **3**, 1413
3 Retting, W. *Colloid Polym. Sci.* 1975, **253**, 852
4 Jones, T. T. *Pure Appl. Chem.* 1976, **45**, 39
5 Gotham, K. V. and Scrutton, I. N. *Polymer* 1978, **19**, 341
6 Puttick, K. E. *J. Phys. D.-Appl. Phys.* 1978, **11**, L69
7 Lindsay, S. M., Hartley, A. J. and Shepherd, I. W. *Polymer* 1976, **17**, 501
8 Hennig, J. *Kunstoffe* 1967, **57**, 385
9 Robertson, R. E. and Buenker, R. J. *J. Polym. Sci.* 1964, **A-2**, 4889
10 Wright, H. Faraday, C. S. N., White, E. F. T. and Treloar, L. R. G. *J. Phys. D.-Appl. Phys.* 1971, **4**, 2002
11 Donald, A. M. and Kramer, E. J. *Phil. Mag.* in press
12 Berry, J. P. *J. Polym. Sci.* 1961, **50**, 313
13 Murray, J. and Hull, D. *Polymer* 1969, **10**, 451
14 Hull, D. *J. Mater. Sci.* 1970, **5**, 357
15 Kambour, R. P. *J. Polym. Sci. Macromol. Rev.* 1973, **7**, 1
16 Beahan, P., Bevis, M. and Hull, D. *Phil. Mag.* 1971, **24**, 1267
17 Brown, H. R. and Ward, I. M. *Polymer* 1973, **14**, 469

18 Doyle, M. J., Maranci, A., Orowan, E. and Stork, S. T. *Proc. Roy Soc.* 1972, **A329**, 137
19 Rabinowitz, S. and Beardmore, P. *Crit. Rev. Macromol. Sci.* 1972, **1**, 1
20 Harris, J. S. and Ward, I. M. *J. Mater. Sci.* 1970, **5**, 573
21 Thomas, L. S. and Cleereman, K. J. *SPE J.* 1972, **28**, 61
22 Beardmore, P. and Rabinowitz, S. *J. Mater. Sci.* 1975, **10**, 1763
23 Lauterwasser, B. D. and Kramer, E. J. *Phil. Mag.* 1979, **A39**, 469
24 Sneddon, I. N. 'Fourier Transforms', McGraw-Hill, New York, 1951, 395
25 Bilby, B. A. and Eshelby, J. D. 'Dislocations and the Thoery of Fracture' in 'Fracture', Vol 1, (Ed. H. Liebowitz) Academic Press, New York, 1972, 111
26 Kramer, E. J. in 'Developments in Polymer Fracture', (Ed. E. H. Andrews) Applied Science, Barking, England, 1979, 55
27 Hirth, J. P. and Lothe, J. 'Thoery of Dislocations', McGraw-Hill, New York, 1968, 398
28 Brown, H. R. and Kramer, E. J. *J. Macromol. Sci.* (*B*) in press